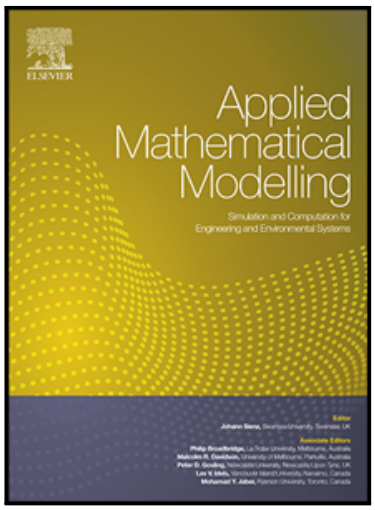

Multi-objective optimization algorithm for analysis of hardened steel turning manufacturing process

Leandro Framil Amorim , Anderson Paulo de Paiva ,
Pedro Paulo Balestrassi , João Roberto Ferreira

PII: S0307-904X(22)00079-8
DOI: https://doi.org/10.1016/j.apm.2022.02.011
Reference: APM 14406

To appear in: *Applied Mathematical Modelling*

Received date: 19 October 2021
Revised date: 11 February 2022
Accepted date: 13 February 2022

Please cite this article as: Leandro Framil Amorim , Anderson Paulo de Paiva , Pedro Paulo Balestrassi , João Roberto Ferreira , Multi-objective optimization algorithm for analysis of hardened steel turning manufacturing process, *Applied Mathematical Modelling* (2022), doi: https://doi.org/10.1016/j.apm.2022.02.011

Highlights:

- Cost and tool life of a hardened steel turning of are properly characterized as typical Poisson random variables.
- Objective functions are simultaneously optimized coupled with their respective variances.
- The proposed method reduces the dimension of the Multi-Objective Optimization problem.
- Proposed Confidence ellipse for Pareto points supports a decision-making based on variability and mean shift.
- A multivariate robust setup for steel turning process is obtained according to the Fuzzy decision-maker.

Multi-objective optimization algorithm for analysis of hardened steel turning manufacturing process

Leandro Framil Amorim [1, *], Anderson Paulo de Paiva [1], Pedro Paulo Balestrassi [1], João Roberto Ferreira [1]

[1] Institute of Industrial Engineering and Management, Federal University of Itajubá, Minas Gerais, Brazil.

* Corresponding author. E-mail address: leandroframorim@gmail.com (L.F. Amorim)

Declarations of interest: None

Abstract: This paper presents a multi-objective optimization algorithm that combines Normal Boundary Intersection method with response surface models of equimax rotated factor scores in order to simultaneously optimize multiples sets of means and variances of manufacturing processes characteristics. The algorithm uses equimax factor rotation to separate means and variances in individual and uncorrelated functions and afterwards combines them in a mean squared error function. These functions are then optimized using Normal Boundary Intersection method generating a Pareto frontier. The optimal solutions found are then filtered according to a 95% non-overlapping confidence ellipses for the predicted values of the responses and posteriorly they are assessed by a Fuzzy decision-maker index established between the volume of each confidence ellipsoid and the Mahalanobis distance between each Pareto point and its individual optima for a given weight. In order to illustrate the practical implementation of this approach, two cases involving the multi-objective optimization of the hardened steel turning process were considered: (a) the AISI 52100 hardened steel turning with CC6050 mixed ceramic inserts and (b) the AISI H13 hardened steel turning with CC 670 mixed ceramic tools. For both cases, the best setup for cutting speed (V), feed rate (f) and depth of cut (d) were adjusted to find the minimal process cost (K_p) and the maximal tool life (T), both responses with minimal variance. The suitable results achieved in these case studies indicate that the proposal may be useful for similar manufacturing processes.

Keywords: Multi-objective Optimization, Normal Boundary Intersection, Factor Analysis, Confidence Ellipse.

Nomenclature

$f_i(\mathbf{x})$	i-th objective function
$g_i(\mathbf{x}) \le 0$	inequality constraint
$h_i(\mathbf{x}) = 0$	equality constraint
$\mathbf{x}, \mathbf{x}^T = [x_1, x_2, \ldots, x_k]$	solution vector or design vector
$\boldsymbol{\Omega}$	solution space
$\mathbf{x}^T\mathbf{x} \le \rho^2$	constraint representing the spherical region of a CCD design
ρ	radius of the spherical region
k	CCD design parameters or factors
m, p	number of objective functions or response (output) variables
n	number of experimental runs
r	number of coefficients in the regression models except β_0
$\mathbf{X}_{(n \times r+1)}$	design matrix derived from CCD with n rows and r+1 columns
CCD	Central Composite Design (Rotatable)
$\mathbf{Y}, \mathbf{Y}=[\mathbf{y}_1, \mathbf{y}_2, \ldots, \mathbf{y}_p]$	matrix of response variables
$\boldsymbol{\beta}, \boldsymbol{\beta}^T = [\beta_0, \beta_1, \ldots, \beta_k]$	vector of coefficients of the regression models
$\boldsymbol{\Phi}$	Payoff matrix
$\overline{\boldsymbol{\Phi}}$	scaled (or normalized) form of Payoff matrix
$\mathbf{n}$	Quasi-normal vector
$\overline{\mathbf{F}}(\mathbf{x})$	vector of scaled objective functions
$\overline{f}_i(\mathbf{x})$	Individual scaled objective function
f_i^U	Utopia value for $f_i(\mathbf{x})$
f_i^N	Nadir value for $f_i(\mathbf{x})$
MSE	Mean Square Error
T_i	Target value for $f_i(\mathbf{x})$
$\hat{\sigma}_i^2(\mathbf{x})$	estimated variance equation
MMSE	Multivariate Mean Square Error
$PC_i(\mathbf{x})$	response surface model for the i-th principal component score
ξ_{PCi}	Target for principal component regression model
λ_i, e_i	eigenvalue and eigenvector
Z	Standardized normal variable Z~N(0, 1)
$\mathbf{w}, \mathbf{w}^T = [w_1, w_2, \ldots, w_p]$	vector of weights for multiobjective optimization

	mean square error of the i-th response surface
	predicted standard deviation for the ith response
	proportion of explained variance of residuals
Σ, **R**	Variance-covariance and correlation matrices of order p x p
ℓ_{pm}	Factor loadings (weighted eigenvectors of **Σ** or **R**)
	Loading vector (p x p)
	Variance-covariance matrix of errors
$\mathbf{z_0(x_0)}$	Positional vector relative to the solution space
	$\mathbf{z_0^T} = \left[\, 1 \;\; x_1 \;\; x_2 \;\; x_3 \;\; x_1^2 \;\; x_2^2 \;\; x_3^2 \;\; x_1x_2 \;\; x_1x_3 \;\; x_2x_3 \,\right]$
$MSE(FA)_i(\mathbf{x})$	Mean square error function for rotated factor scores
$FA_{\mu_i(T)}(\mathbf{x})$	Response surface model for the rotated factor score of mean
$FA_{\sigma_i^2(T)}(\mathbf{x})$	Response surface model for the rotated factor score of variance
$T_{FA_{\mu_i(T)}}$	Target value for $FA_{\mu_i(T)}(\mathrm{x})$
$MSE(FA)_i^U$	Utopia value for $MSE(FA)_i(\mathbf{x})$
$MSE(FA)_i^N$	Nadir value for $MSE(FA)_i(\mathbf{x})$
s	number of selected fators ($s \le p$)
$\mathbf{W}_{n\mathbf{x}n}$	diagonal matrix of weights
V	Volume of a confidence ellipse
Γ(.)	Gamma function
S	Sample variance-covariance matrix (p x p)
MD	Mahalanobis distance
T	Tool life
Kp	Total cost of manufacturing process
V	Cutting Speed (m/min)
f	Feed rate (mm/rev)
d	Depth of cut (mm)
μ^T	Fuzzy decision maker
NBI	Normal Boundary Intersection
OLS	Ordinary Least Squares
MWLS	Multivariate Weighted Least Squares
DOE	Design of Experiments
POE	Propagation of Error

1. Introduction

For a large deal of manufacturing systems, the vital assignment in engineering is to ensure legitimately stable results, as many standardized products as possible. As an initial way to model these systems to be able to control it aiming at the optimal result, researchers have employed design of experiment (DOE) arrays to simultaneously optimize multiple quality characteristics adjusting the process parameters to their best levels. Examples of such approach can be seen in several manufacturing processes like resistance spot welding [1], pulsed gas metal arc welding [2], electro discharge machining [3], hardened steel turning [4-6], free steel machining [7, 8], end milling [9] among others.

On this wise, the quality of products will only be assured if expected values of the performance characteristics are near to their targets, with the least possible dispersion [10]. Eventual mean shifts and an excess of variance are typically occasioned by an inadequate setting of control variables or even by the presence of noise variables [11] and it is particularly observed in mass production lines [12]. In order to increase the product's quality, researchers must minimize, simultaneously, the mean shift and the process variance, discovering the levels of the process control variables that provide an acceptable trade-off between both low variance and a deviation from a previously targeted mean [13]. If there is just one characteristic of interest and if the researcher considers different weights for mean and variance, the problem may be solved by any bi-objective optimization method [12].

Sometimes, it is convenient to use the MSE objective function as a way to agglutinate mean and variance around a specific target for the characteristic of interest [13]. Thusly, it becomes possible to synchronously optimize the process accuracy and precision, concurrently optimizing centrality and dispersion of a process performance variable subject to its respective constraints.

Expanding this reasoning to multi-objective optimization, several works have been carried out considering the simultaneous optimization of several characteristics of processes and their respective variances treating these functions as individual objectives in a goal programming approach [14] or replacing the mean and variance functions directly by MSE indexes [15]. In both cases, the variances are computed from pure replicates [16], residuals from mean models [17], crossed arrays [8] or combined arrays [9]. The aforementioned schemes of computing variance have different costs and precision depending on the number of experiments required, and their use in practice depends on the researcher´s available budget [12].

As a traditional multiobjective optimization method, Normal Boundary Intersection method (NBI) have been also successfully used to solve mean-variance optimization problems in the context of machining process like AISI 12L14 steel turning [8] or AISI 1045 end milling [9]. This method was specifically developed to generate a uniform spread of the Pareto frontier, even in a non-convex solution region [18]. The importance and flexibility inherent to this technique are featured in studies such as [19], in which its strength and suitability were extensively investigated according to the optimization of different and complex types of systems. Pareto frontier is a set of feasible, optimal and nondominated solutions that allows the decision maker to choose the best vector of parameters capable of providing a high level of quality for a specific process of interest [18]. When applied to MSE problems, Pareto frontier presents the feasible solutions found during the trade-off process between mean and variance objective functions. The complexity of problem increases as more objective functions are considered. In this way, for two characteristics there will be four objective functions – being two mean equations and two variance equations; if mean and variance are agglutinate as a MSE index, there will be just two dimensions to the multiobjective problems. Therefore, depending on the scheme adopted to treat the dual mean-variance, larger will be the number of sub-problems involved in the optimization routine [19].

Correlation is also an important aspect to be considered in multiobjective optimization [20] since its negligence may compromises the final results: for example, when two positively correlated objective functions with different sense of optimization are simultaneously optimized the antagonist weights used in a convex combination will change the original correlation signal, creating a set of unrealistic solutions. Besides, since most of multiobjective optimization methods depends on the anchor points to promote normalization or scalarization, their definition based on individual optimization, neglecting the variance-covariance structure of the response data, will originate unrealistic optimization results. The influence of correlation over the optimization results has been faced with several different approaches, as follows: (a) those methods based on the computation and modelling of the correlation of each experiment like as in [21], (b) those considering the variance-covariance matrix of response data to compose a multivariate distance between the vector of expected values and their respective targets [22], (c) those using directly Principal Component Analysis (PCA) to develop latent variables capable of replace the original correlated responses [20] or to create multivariate mean square error indexes [23] and (d), those methods using rotated factor scores (FA) to create uncorrelated objective functions or even relative indexes [24]. It is straightforward that approaches considering the computation of correlation or the covariance

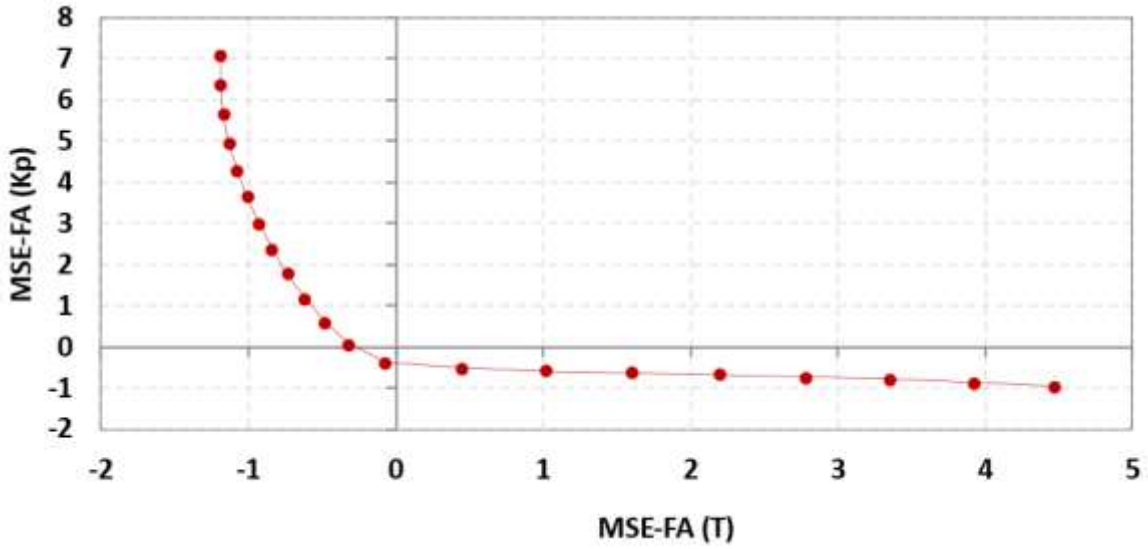

Fig. 4 - Pareto frontier of **$MSE(FA)_1(T)$** and **$MSE(FA)_2(K_P)$**.

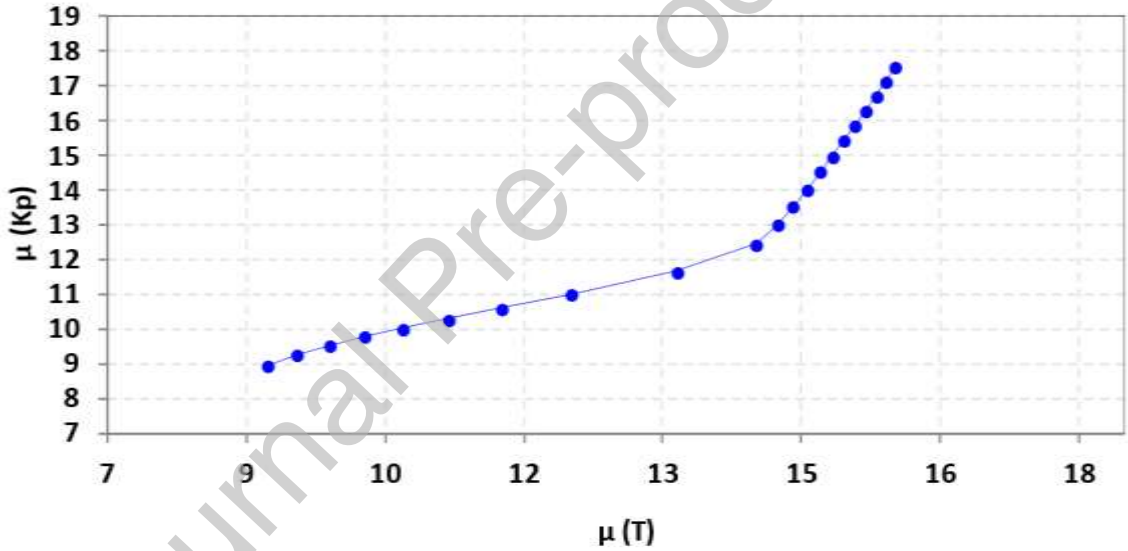

Fig. 5 - Observed values of μ(T) and μ(K_p) from the NBI (MSE-FA) Pareto frontier.

Table 8 presents the results relative to the procedure established at the **Step 5**. Firstly, the Mahalanobis distance between the frontier vectors and their individual targets are calculated. The targets used were μ(T) for T* = 17.505 and μ(K_p) for K_p* = 6.328; MD was determined using the variance-covariance matrix **S** of each solution.

Secondly, 95% confidence ellipses are formed for each Pareto solution and are plotted considering the mean vector as their respective centroids (**Fig. 6)**. Note in this part that all ellipses are based on the variance-covariance matrix, consequently their eigenvalues and eigenvectors are repeated. The center of each ellipse are the pairs resulting from the *μ(T)* and *μ(K_p)* frontier.

Table 8 - Results of Pareto frontier for **MSE(FA)$_1$ (T)** and **MSE(FA)$_2$ (K_p)**.

w_1	FA_4 $\mu(K_p)$	FA_2 $(\sigma^2(K_p))$	FA_3 $(\sigma^2(T))$	FA_1 $(\mu(T))$	MD	V	μ_M	μ_V	Fuzzy (μ^T)
0.00	-1.04	-1.10	0.11	-0.01	10,419.5	0.00248	0.9083	1.00	0.922
0.05	-1.02	-1.02	-0.04	-0.10	21,983.4	0.00125	0.8064	1.00	0.835
0.10	-1.01	-0.95	-0.17	-0.22	8,565.2	0.00336	0.9246	1.00	0.936
0.15	-1.02	-0.89	-0.28	-0.35	9,851.8	0.00301	0.9133	1.00	0.926
0.20	-1.03	-0.83	-0.37	-0.50	17,823.6	0.00171	0.8431	1.00	0.867
0.25	-1.03	-0.77	-0.43	-0.67	91,566.6	0.00034	0.1932	1.00	0.314
0.30	-1.04	-0.72	-0.48	-0.87	31,607.5	0.00104	0.7216	1.00	0.763
0.35	-1.02	-0.66	-0.49	-1.13	22,688.6	0.00156	0.8002	1.00	0.830
0.40	-0.95	-0.60	-0.43	-1.50	113,488.3	0.00036	0.0000	1.00	0.150
0.45	-0.76	-0.36	-0.43	-1.76	22.6	2.46341	0.9999	0.46	0.918
0.50	-0.58	-0.07	-0.57	-1.80	17.1	3.61246	1.0000	0.20	0.880
0.55	-0.41	0.18	-0.70	-1.81	15.5	4.18781	1.0000	0.08	0.861
0.60	-0.24	0.40	-0.81	-1.82	14.9	4.45941	1.0000	0.02	0.852
0.65	-0.07	0.60	-0.92	-1.82	14.7	4.52992	1.0000	0.00	0.850
0.70	0.09	0.77	-1.01	-1.81	14.8	4.45143	1.0000	0.02	0.853
0.75	0.25	0.91	-1.10	-1.80	15.0	4.25345	1.0000	0.06	0.859
0.80	0.40	1.03	-1.18	-1.78	15.4	3.95292	1.0000	0.13	0.869
0.85	0.55	1.13	-1.24	-1.76	16.1	3.55805	1.0000	0.21	0.882
0.90	0.70	1.21	-1.29	-1.74	17.0	3.06848	1.0000	0.32	0.898
0.95	0.85	1.27	-1.33	-1.72	18.4	2.47030	1.0000	0.45	0.918
1.00	1.00	1.30	-1.36	-1.68	21.5	1.70931	0.9999	0.62	0.943

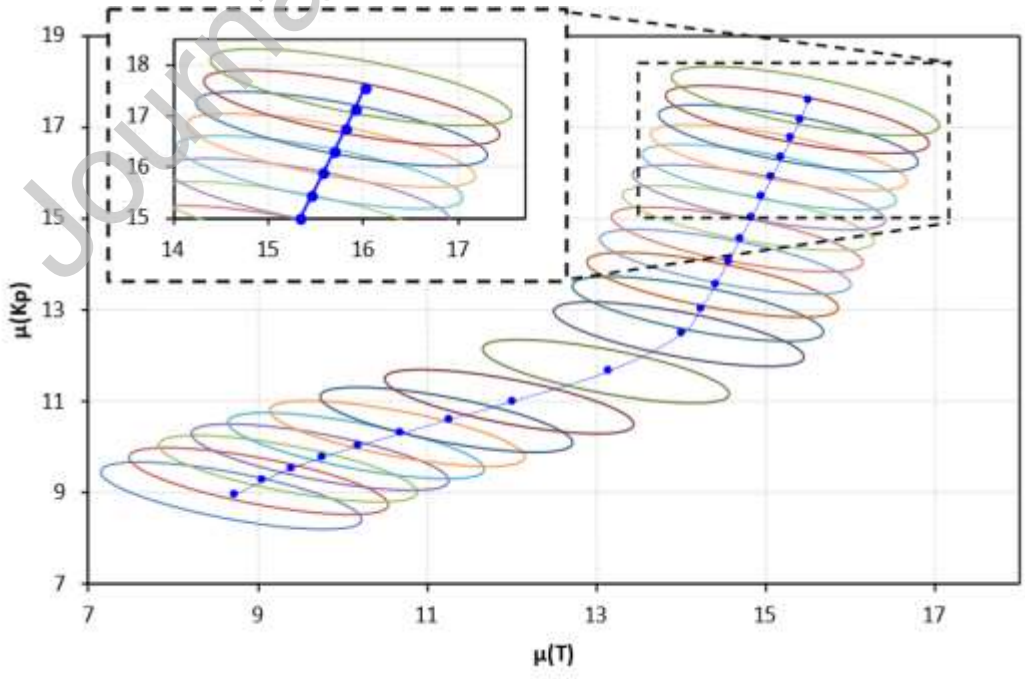

Fig. 6 - Confidence Ellipse for Pareto frontier of **MSE$_1$(T)** and **MSE$_2$(K_P)**.

Complementing the routine of **Step 5**, the volume of each ellipse is calculated using p = 2 and n = 7. In order to obtain 95% confidence ellipses (α=0.05), Eq. (26) is applied to two responses (T and K_p) m = 2, which has a CCD design with 18 observations (n) and response models have 9 coefficients each (r), except for the constant term, as in Eq. (26).

$$\begin{bmatrix} \mathbf{z}_i^{\mathrm{T}}\hat{\boldsymbol{\beta}}(\mathrm{T})_{\mathrm{MWLS}} \\ \mathbf{z}_i^{\mathrm{T}}\hat{\boldsymbol{\beta}}(\mathrm{K_p})_{\mathrm{MWLS}} \end{bmatrix} + \sqrt{\frac{2}{18-9-2}F_{2,5}(0.05)\left[\mathbf{z}^{\mathrm{T}}(\mathbf{x}_i)\left(\mathbf{X}^{\mathrm{T}}\mathbf{W}\mathbf{X}\right)^{-1}\mathbf{z}(\mathbf{x}_i)\right]} \times \begin{bmatrix} 14.236 & 0 \\ 0 & 1.264 \end{bmatrix} \times \begin{bmatrix} 0.937 & 0.351 \\ -0.351 & 0.937 \end{bmatrix} \times \begin{bmatrix} \cos\phi \\ \sin\phi \end{bmatrix} \quad (26)$$

$$\mathbf{n}\hat{\boldsymbol{\Sigma}} = \begin{bmatrix} \left(\mathbf{res}_{\mathrm{T}}\right)^{\mathrm{T}}\mathbf{res}_{\mathrm{T}} & \left(\mathbf{Cov}_{\mathbf{res}_{\mathrm{T}}\times\mathbf{res}_{\mathrm{K_p}}}\right)^{\mathrm{T}}\mathbf{Cov}_{\mathbf{res}_{\mathrm{T}}\times\mathbf{res}_{\mathrm{K_p}}} \\ \left(\mathbf{Cov}_{\mathbf{res}_{\mathrm{T}}\times\mathbf{res}_{\mathrm{K_p}}}\right)^{\mathrm{T}}\mathbf{Cov}_{\mathbf{res}_{\mathrm{T}}\times\mathbf{res}_{\mathrm{K_p}}} & \left(\mathbf{res}_{\mathrm{K_p}}\right)^{\mathrm{T}}\mathbf{res}_{\mathrm{K_p}} \end{bmatrix} = \begin{bmatrix} 12.634 & -4.268 \\ -4.268 & 2.866 \end{bmatrix} \quad (27)$$

Note that the eigenvalues and eigenvectors used are derived from variance-covariance matrix , which consists of the relationship between regression residuals of T and K_p). The variance and covariance associated with each point are represented by the ellipse formed, which expresses the uncertainty of that solution found.

In **Step 6**, the membership functions for MD and confidence ellipses volume are calculated. The corresponding values of utopia (1) and nadir (0) are respectively: 14.7 and 113,488.3 for μ_M, 0.00034 and 4.530 for μ_V. Subsequently, with weight of 85/15 between the membership functions, the best value for the Fuzzy decision maker is 0.943 (higher).

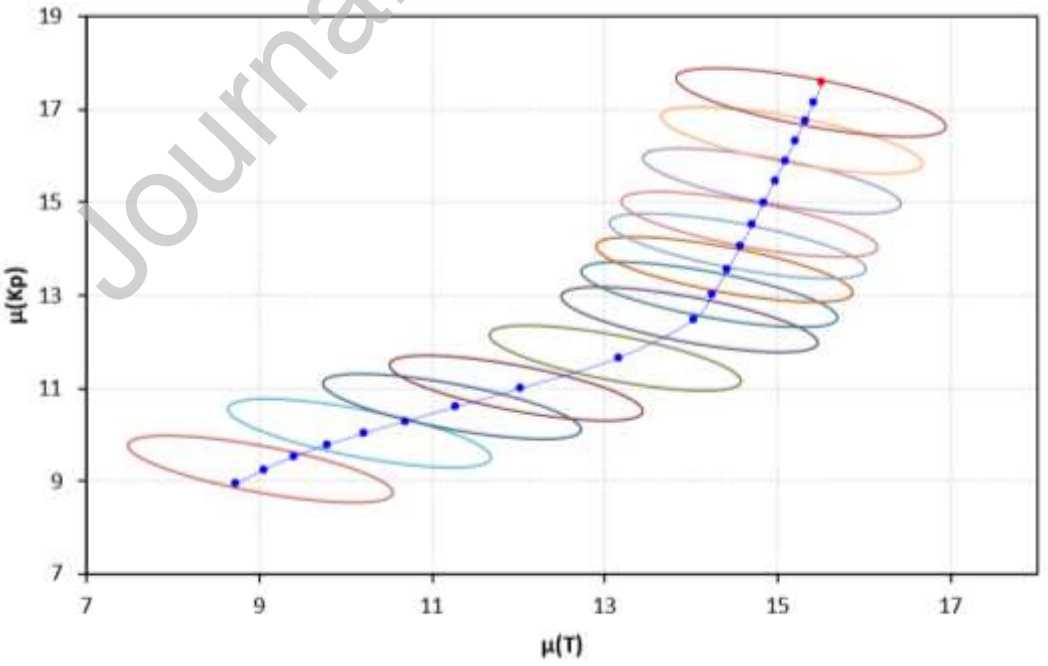

Fig. 7 - Non-Overlapping Confidence Ellipses in Pareto frontier

Therefore, this solution found is point 21 (w=1.0), with cutting speed (V) = 220.4 m/min, Feed rate (f) =0.209 mm/rev and Depth of cut (d) = 0,340 mm. This configuration will promote an expect tool life $\mu(T)$ = 15.51 min and a process cost about $\mu(K_p)$ = 17.57 US$/piece.

Finally, after removing the overlapping ellipses, it is obtained the filtered Pareto frontier shown in the **Fig. 7**. Therefore, this procedure reduces from 21 to 13, the number of optimal scenarios in practice.

The results achieved were better than those achieved by [4], which were: Multivariate optimization K_p = 7.284 US$/piece and T = 5.637 min; Multiple Optimization K_p = 7.410 US$/piece and T = 6.000 min. In both cases, the solution found has a worse relationship between the cost per part (K_p) and the tool life (T).

5.2. Multiobjective optimization of AISI H13 hardened steel turning.

In a similar process of manufacturing hardened steel turning, the same variables are modeled to demonstrate the viability of the proposed method. Although the CCD has the same three input variables (V, f, d), only 2 of the 8 process output responses, tool life (T) and total cost (K_p) are selected for this example. Further information about process data can be found in [5].

The CCD characteristics are: 3 factors, 1 replicate, 19 runs, being 8 cube points, 5 center points in cube, 6 axial points, 0 center points in axial and the distance of each axial point α = 1.68179. **Table 9** represents the DOE of this second case.

The correlation measured between variables T and K_p presents a Pearson coefficient equal to 0.758 (p-value = 0.000). Therefore, it is statistically significant, which is justified for the continuation of **Step 2**.Also analogous to the first numerical example, PCFA is performed for T, K_p, $\sigma^2(T)$ and , extracting four factors using principal component and Equimax rotation (**Table 10**).

From **Table 10** it is possible to verify that FA_4 replaces μ(T) and presents a negative correlation with this variable; therefore, the minimization of FA_4 leads to the maximization of tool life; FA_3 is positively correlated with σ^2 (T), then its minimization reduces the variance of tool life. FA_1 and FA_2 are positively correlated with $\mu(K_p)$ and σ^2 (K_p), respectively; both minimization reduces the process costs and its respective variances.

Table 9 - Cutting parameters and responses for the CCD 2nd case

Runs	*V*	*f*	*d*	*T*	K_p	$\sigma^2(T)$	
1	100.00	0.100	0.150	59.50	2.99	33.4	1.008
2	225.00	0.100	0.150	35.50	1.87	4.7	1.012
3	100.00	0.225	0.150	50.50	2.60	1.4	1.003
4	225.00	0.225	0.150	31.00	1.65	16157.5	1.022
5	100.00	0.100	0.330	60.00	3.97	2535.5	1.034
6	225.00	0.100	0.330	29.50	2.31	1.5	1.001
7	100.00	0.225	0.330	50.50	3.33	5.5	1.008
8	225.00	0.225	0.330	29.50	1.41	317.3	1.001
9	57.39	0.163	0.240	59.00	4.20	309.2	1.018
10	267.61	0.163	0.240	28.00	1.48	2970.2	1.005
11	162.50	0.057	0.240	38.00	3.44	27101.7	1.044
12	162.50	0.268	0.240	40.00	1.94	578672.3	1.020
13	162.50	0.163	0.089	49.25	1.81	1.1	1.001
14	162.50	0.163	0.391	48.00	2.56	1.1	1.000
15	162.50	0.163	0.240	44.50	2.57	1.3	1.001
16	162.50	0.163	0.240	44.00	2.54	1.3	1.001
17	162.50	0.163	0.240	45.00	2.61	1.3	1.001
18	162.50	0.163	0.240	45.50	2.53	1.3	1.001
19	162.50	0.163	0.240	44.50	2.50	1.3	1.001

Source: Adapted from Campos [27]

Table 10 - Sorted Rotated Factor Loadings for 2nd case.

	Loadings			
Variable	FA_1	FA_2	FA_3	FA_4
μ(T)	0.433	-0.121	-0.125	**-0.884**
$\mu(K_p)$	**0.915**	-0.034	-0.031	-0.400
σ^2 (T)	-0.039	0.652	**0.744**	0.140
σ^2 (K_p)	-0.053	**0.756**	0.640	0.125
Variance	1.0302	1.0129	0.9798	0.9771
% Var	0.258	0.253	0.245	0.244

Table 11 - Full quadratic models for each response 2nd case

Term	T	K_p	$\sigma^2 K_p$	$\sigma^2 T$	$FA_{1\ \mu(Kp)}$	$FA_{2\ \sigma^2(Kp)}$	$FA_{3\ \sigma^2(T)}$	$FA_{4\ \mu(T)}$
Constant	44.720	2.552	0.001	0.239	0.030	-1.204	-0.524	0.141
V	-10.774	-0.749	0.674	1.104	-0.604	-0.046	0.130	0.948
f	-1.438	-0.342	0.793	1.081	-0.515	0.191	0.123	-0.125
d	-0.666	0.232	0.669	1.073	0.433	0.096	0.187	0.235
V^2	-0.509	0.090	2.004	3.261	0.144	0.151	0.761	0.008
f^2	-2.100	0.037	3.004	3.951	0.169	1.048	0.137	0.151
d^2	1.303	-0.141	0.757	0.725	-0.344	0.476	-0.170	-0.354
*V*f*	1.750	-0.011	1.538	2.804	-0.173	-0.170	0.975	-0.387
*V*d*	-1.000	-0.189	0.365	0.594	-0.278	-0.002	0.157	-0.046
*f*d*	0.500	-0.116	0.914	1.210	-0.234	0.290	0.106	-0.235
R^2 *(adj.)*	92.42	96.74	99.87	99.90	94.22	100.00	99.39	95.55

Table 11 shows the full quadratic models for original responses and respective equimax rotated factor scores. All models present suitable values for R^2 adj. Proceeding to **Step 3**, GRG algorithm are used for calculate the targets for the MSE's functions, nonlinear constraint $\mathbf{x}^T\mathbf{x} \leq 2.828$ (CCD axial distance (ρ) = 1.68179 for k = 3). The result found is **MSE_1 (T)** in $T_{FA_{(\mu)4}}$ = -1.964 and to **MSE_2 (K_p)** in $T_{FA_{(\mu)1}}$ = -1.689.

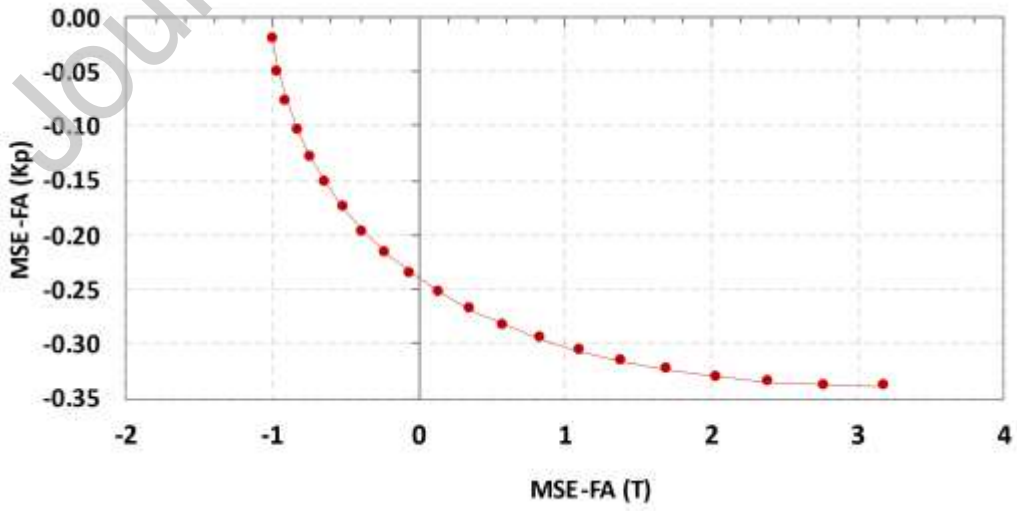

Fig. 8 - Pareto frontier of **MSE_1(T)** and **MSE_2(K_P)** – NBI (MSE-FA) 2nd case

In the **Step 4**, the anchor points are defined as $\mathbf{MSE_1\ (T)}$ = [-0.997, 3.175] and $\mathbf{MSE_2\ (K_p)}$ = [-0.020, -0.339]. NBI method (using GRG) is applied to solve MOP in the MSE of rotated factor scores, forming the Pareto frontier for $\mathbf{MSE_1(T)}$ and $\mathbf{MSE_2(K_p)}$, as in **Fig. 8**. The sequence of mean vectors obtained during the optimization of NBI-RFMSE is plotted in **Fig. 9**.

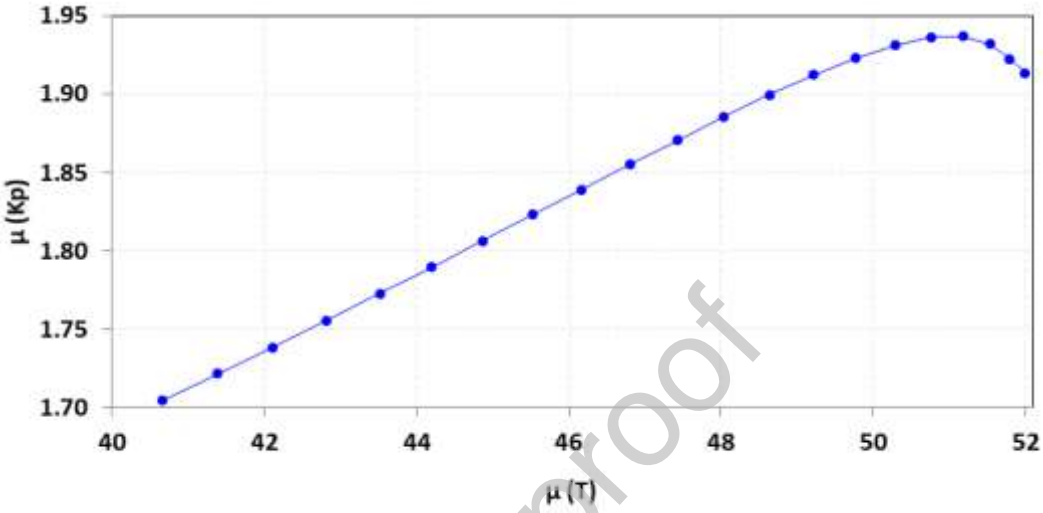

Fig. 9 - Observed values of μ(T) and μ(K_p) from the NBI (MSE-FA) Pareto frontier 2nd case.

After plotting all the confidence ellipses (**Fig. 10**), it is possible to analyze and remove those Pareto points that are overlapping. Of 21 solutions, only 9 remain, as seen in **Fig. 11**. Then, the confidence ellipses volume and MD are calculated with p = 2 and n = 9, using each matrix **S**.

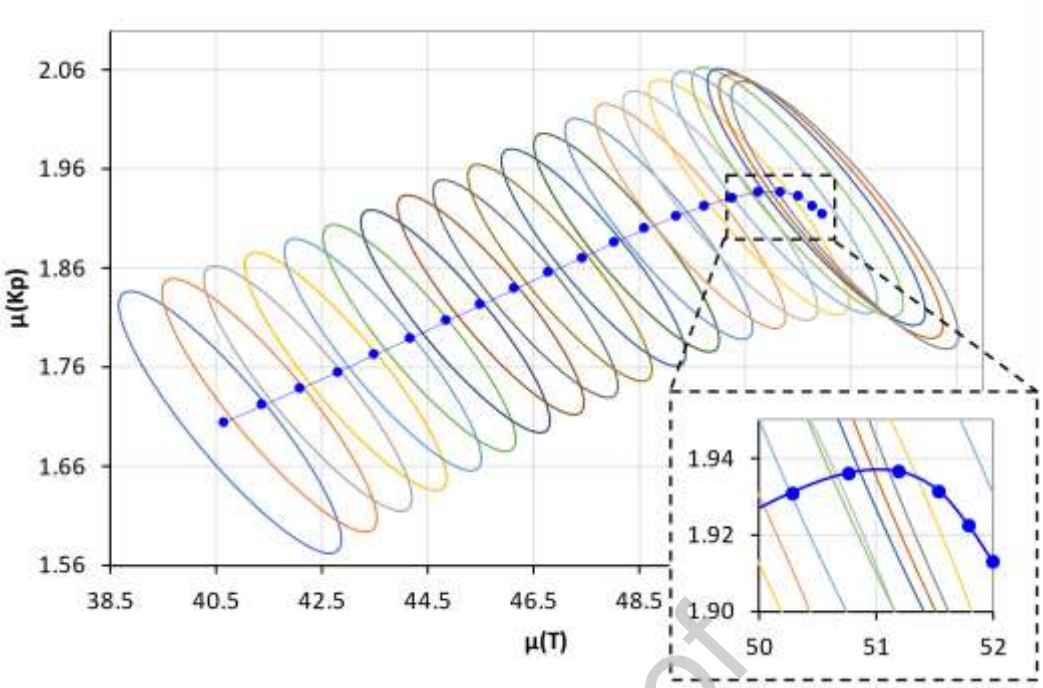

Fig. 10- Confidence Ellipse for Pareto frontier of $\mathbf{MSE_1(T)}$ and $\mathbf{MSE_2(K_P)}$ 2nd case

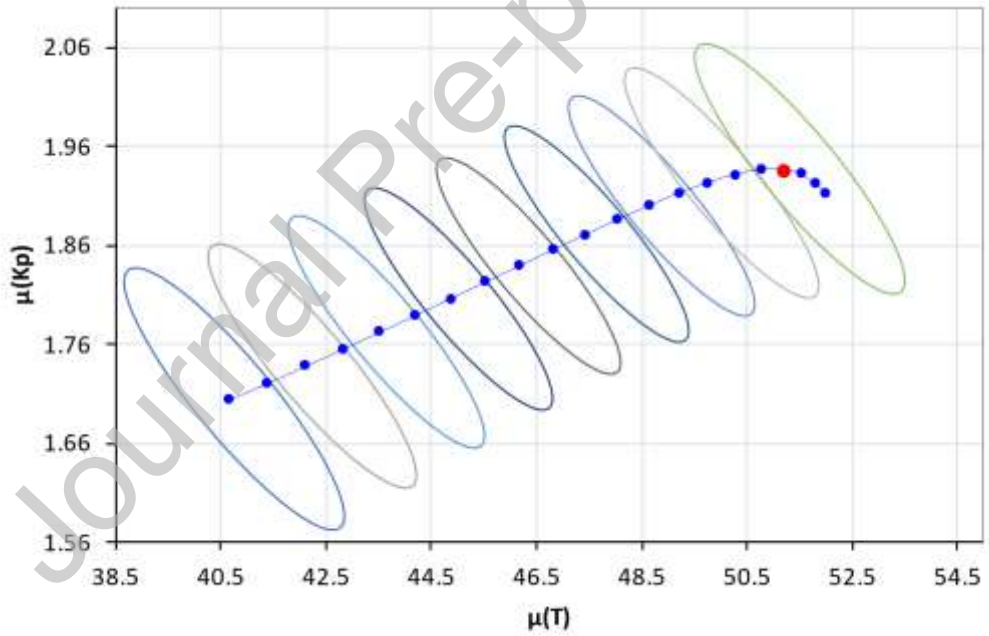

Fig. 11 - Non-overlapping Confidence Ellipses in Pareto frontier 2nd case

Fuzzy decision maker is calculated producing membership functions for MD and V respectively equals to 19.95 and 50.07 for μ_M, 0.87 and 4.83 for μ_V. Given these data, the best overall performance found by decision maker Fuzzy is μ^T = 0.811, relative to the optimum solution point 18 ($w_{1=}$ 0,85), which corresponds to the process settings of Cutting Speed (V) = 178.9 m/min, Feed (f) =0.157 mm/rev and Depth of cut (d) = 0,383 mm. In this way, the

respective response values are μ(T) = 51.18 min for the mixed ceramic tool life and μ(K_p) = 1.94 US$/piece for the process cost.

Table 12 - Comparisons among several multi-objective methods

MOP Method	T	Distance	K_p	Distance
Proposed Method	**51.18**	**11.24**	**1.94**	**0.61**
NBI-MMSE*	50.01	12.41	3.29	1.97
NBI*	37.34	25.08	2.34	1.02
WSUM-MMSE*	49.64	12.78	3.26	1.94
MCG-MMSE*	48.16	14.26	2.63	1.31
AHL-MMSE*	50.48	11.94	3.33	2.01
Target	**62.43**		**1.32**	

As a matter of comparison, the multiobjective optimization of this second case study was repeated with several different algorithms available: (a) the NBI-MMSE method like described in Eq. (7), (b) the traditional NBI in four dimensions (NBI*), (c) the method of weighted sums with MMSE functions (WSUM-MMSE*), (d) the Global criterion method (MCG-MMSE*) and the Arc homotopic length (AHL-MMSE*), both with multivariate mean square error function of Eq. (7). These results are summarized in **Table 12**.

As can be noticed, NBI-RFMSE method outperformed all other strategies in this case which suggests that it may be safety used in the optimization of similar manufacturing process.

5. Conclusions

This paper has presented a multi-objective optimization algorithm that combined the characteristics of the Normal Boundary Intersection method with response surface models of equimax rotated factor scores. This hybrid NBI-RFMSE approach allowed the definition of a MSE function using the uncorrelated functions traced for means and variances for each original response of interest. These new objective functions were then optimized using Normal Boundary Intersection method and generated an equispaced Pareto frontier. For each point of this frontier, were established a 95% confidence ellipse based on its respective variances, covariance and expected value. Solutions with overlapped ellipses were removed from the frontier and afterward, they were assessed in terms of their volume (precision) and

accuracy, using a Fuzzy decision-maker index as a matter of balance the both criteria and the decision maker´s preference.

The use of equimax rotated factor scores have presented some advantages over principal components mainly when compared with NBI-MMSE approach: the first one was the ability to fully separate the objective functions – characteristic that was not be achieve with PCA. From an optimization perspective, such separation allows the influence of the weights to be better transmitted to the objective functions. The second advantage is related to the capacity that the rotation method has to undid the conflict between the sense of optimization of the original variable and the response surface model of the factor scores. Equimax method has also presented the advantage to create decomposed functions with the same degree of explanation of total variance observed in the response data. This feature, that was not observed in PCA scores, allowed the definition of functions with the same degree of importance before the weighting process promoted by the interactions of the NBI algorithm.

The use of 95% confidence ellipses proved to be a suitable approach in filtering the initial Pareto optimal solutions, reducing the number of the alternatives for posterior assessment. As the most innovative proposal of this work, this step brought the concept of statistical independence to the context of optimization, discussions which are so rare in the literature.

Two numerical examples were developed to test the approach. In the case of the multi-objective optimization of the turning process of the AISI 52100 hardened steel carried out with CC6050 mixed ceramic inserts the minimal process cost, the maximal tool life, and minimal variance for both responses were achieved with a cutting speed equal to 220.4 m/min, feed rate equal to 0.209 mm/rev and depth of cut equal to 0,340 mm. This configuration will promote an expect tool life of 15.51 with a variance of 0.09 and a process cost about 17.57 US$/piece, with a variance of 2.09. For AISI H13 hardened steel with CC 670 mixed ceramic tools, similar results were achieved with a cutting speed equal to 178.9 m/min, feed rate equal to 0.157 mm/rev and depth of cut equal to 0.383 mm, setup responsible for a tool life of 51.18 min, with a variance of 0.44 and a process cost around 1.94 US$/piece, with a variance of 0.89. It is worth mentioning that the great difference between T and Kp in the numerical cases is due to differences in the type of inserts and in the cost of the steels used.

The quality of these practical results motivates us to suggest the method may be extended to applications on multi-objective optimization problems of many others manufacturing processes.

Acknowledgement: The authors would like to express their gratitude to National Council for Scientific and Technological Development (CNPq), Coordination for the Improvement of Higher Education Personnel (CAPES), Research Support Foundation of Minas Gerais State (FAPEMIG) and Federal University of Itajubá (UNIFEI) for their support in this research.

References

[1] X. Cao, Z. Li, X. Zhou, Z. Luo, J. Duan, Modeling and optimization of resistance spot welded aluminum to Al-Si coated boron steel using response surface methodology and genetic algorithm, Measurement 171 (2021) 108766. https://doi.org/10.1016/j.measurement.2020.108766

[2] Paiva, A.P., Costa, S.C., Paiva, E.J., Balestrassi, P.P., Ferreira, J.R., Multi-objective optimization of pulsed gas metal arc welding process based on weighted principal component scores, Intl. J. Adv. Manuf. Tech. 50 (2010) 113-125. https://doi.org/10.1007/s00170-009-2504-y

[3] P. Sharma, D. Chakradhar, S. Narendranath, Measurement of WEDM performance characteristics of aero-engine alloy using RSM-based TLBO algorithm, Measurement 179 (2021) 109483. https://doi.org/10.1016/j.measurement.2021.109483

[4] A.P. Paiva, J.R. Ferreira, P.P. Balestrassi, A multivariate hybrid approach applied to AISI 52100 hardened steel turning optimization, J. Mater. Process. Technol. 189 (2007) 26-35. https://doi.org/10.1016/j.jmatprotec.2006.12.047

[5] J.H.D. Gaudêncio, F.A. Almeida, R.C. Sabioni, J.B. Turrioni, A.P. Paiva, P.H.S. Campos, Fuzzy multivariate mean square error in equispaced Pareto frontiers considering manufacturing process optimization problems, Eng. Comp. 35 (2019) 1213–1236, https://doi.org/10.1007/s00366-018-0660-0.

[6] L.G.D. Lopes, T.G. Brito, A.P. Paiva, R.S. Peruchi, P.P. Balestrassi, Robust parameter optimization based on multivariate normal boundary intersection, Comput. Ind. Eng. 93 (2016) 55-66. https://doi.org/10.1016/j.cie.2015.12.023

[7] D.M.D. Costa, T.I. Paula, P.A.P. Silva et al., Normal boundary intersection method based on principal components and Taguchi's signal-to-noise ratio applied to the multiobjective optimization of 12L14 free machining steel turning process, Int. J. Adv. Manuf. Technol. 87 (2016) 825–834. https://doi.org/10.1007/s00170-016-8478-7

[8] J.H.D. Gaudêncio, F.A. Almeida, J.B. Turrioni, R.C. Quinino, P.P. Balestrassi, A.P. Paiva, A multiobjective optimization model for machining quality in the AISI 12L14 steel turning process using fuzzy multivariate mean square error, Precis. Eng. 38(3) (2014) 628-638. https://doi.org/10.1016/j.precisioneng.2019.01.001

[9] T.G. Brito, A.P. Paiva, J.R. Ferreira, J.H.F. Gomes, P.P. Balestrassi, A normal boundary intersection approach to multiresponse robust optimization of the surface roughness in end

milling process with combined arrays, Precis. Eng. 56 (2019) pp. 303-320. https://doi.org/10.1016/j.precisioneng.2014.02.013

[10] D.K.J. Lin, W. Tu, Dual response surface optimization, J. Qual. Technol. 27 (1995) 34-39. https://doi.org/10.1080/00224065.1995.11979556

[11] L.C. Tang, K. Xu, A unified approach for dual response surface optimization. J. Qual. Technol. 34 (2002) 437-447. https://doi.org/10.1080/00224065.2002.11980175

[12] G.L. Boylan, P.L. Goethals, B.R. Cho, Robust parameter design in resource-constrained environments: An investigation of trade-offs between costs and precision within variable processes, Appl. Math. Modell. 37 (2013) 2394-2416. https://doi.org/10.1016/j.measurement.2019.07.072

[13] S. Shin, F. Samanlioglu, B.R. Cho, M.M. Wiecek, Computing trade-offs in robust design: perspectives of the mean squared error, Comput. Ind. Eng. 60 (2011) 248-255. https://doi.org/10.1016/j.cie.2010.11.006

[14] J. Kovach, B.R. Cho, A D-optimal design approach to constrained multiresponse robust design with prioritized mean and variance considerations, Comput. Ind. Eng. 57 (2009) 237-245. https://doi.org/10.1016/j.cie.2008.11.011

[15] O. Köksoy, Multiresponse robust design: Mean square error (MSE) criterion, Appl. Math. Comput. 175(2) (2006) 1716-1729. https://doi.org/10.1016/j.amc.2005.09.016

[16] L.G.D. Lopes, T.G. Brito, A.P. Paiva, R.S. Peruchi, P.P. Balestrassi, Robust parameter optimization based on multivariate normal boundary intersection, Comput. Ind. Eng. 93 (2016) 55-66. https://doi.org/10.1016/j.cie.2015.12.023

[17] R.D. Plante, Process capability: a criterion for optimizing multiple response product and process design, IIE Trans. 33 (2001) 497-509. https://doi.org/10.1023/A:1007694030052

[18] I. Das, J.E. Dennis, Normal boundary intersection: A new method for generating the Pareto surface in nonlinear multicriteria optimization problems, SIAM J. Optim. 8 (1998) 631-657. https://doi.org/10.1137/S1052623496307510

[19] A. Ghane-Kanafe, E. Khorram, A new scalarization method for finding the efficient frontier in non-convex multi-objective problems, Appl. Math. Modell. 39 (2015) 7483-7498. https://doi.org/10.1016/j.apm.2015.03.022

[20] N. Bratchell, Multivariate response surface modeling by principal components analysis. J. Chemom. 3(4) (1989) 579-588. https://doi.org/10.1002/cem.1180030406

[21] F.C. Wu, Optimization of correlated multiple quality characteristics using desirability function, Qual. Eng. 17 (2004) 119-126.
https://doi.org/10.1081/QEN-200028725.

[22] A.I. Khuri, M. Conlon, Simultaneous optimization of multiple responses represented by polynomial regression functions. Technometrics. 23 (1981) 363-375.
https://doi.org/10.1080/00401706.1981.10487681

[23] Paiva, A.P., Paiva, E.J., Ferreira, J.R. Balestrassi, P.P. Costa, S.C. A multivariate mean square error optimization of AISI 52100 hardened steel turning, The International Journal of Advanced Manufacturing Technology 43 (2009) 631-643.
http://dx.doi.org/10.1007/s00170-008-1745-5

[24] F.L. Naves, T.I. de Paula, P.P. Balestrassi, W.L.M. Braga, R.S. Sawhney, A.P. Paiva, Multivariate Normal Boundary Intersection based on rotated factor scores: A multiobjective optimization method for methyl orange treatment, J. Clean. Prod. 143 (2017) 413-439.
https://doi.org/10.1016/j.jclepro.2016.12.092

[25] R.A. Johnson, D. Wichern, Applied Multivariate Statistical Analysis, 6th ed. Prentice-Hall, New Jersey, 2007.

[26] R.R. Leite, Normal boundary intersection method for quadratic models of rotated factory scores. Dissertation, Federal University of Itajubá, Brazil, 2019.
https://repositorio.unifei.edu.br/jspui/handle/123456789/1903

[27] P.H.S. Campos, Metodologia DEA-OTS: Uma contribuição para a seleção ótima de ferramentas no Torneamento do Aço ABNT H13 Endurecido. PhD Dissertation, (2015). Federal University of Itajubá, Brazil.
https://repositorio.unifei.edu.br/jspui/handle/123456789/127

[28] E. Zitzler, L. Thiele, M. Laumanns, C.M. Fonseca, V.G. da Fonseca, Performance assessment of multiobjective optimizers: an analysis and review. IEEE Trans. Evol. Comput. 7(2) (2003) 117-132.
https://doi.org/10.1109/TEVC.2003.810758

[29] H.J. Zimmermann, Fuzzy programming and linear programming with several objective functions. Fuzzy Sets Syst. 1 (1978) 45-55.
https://doi.org/10.1016/0165-0114(78)90031-3

[30] R.H. Myers, D.C. Montgomery, G.G. Vining, Generalized Linear Models – With applications in Engineering and the Sciences, Wiley, (2002).